Title

NK cells mediate clearance of CD8+ T cell–resistant tumors in response to STING agonists

Journal

Science Immunology, 5(45)

ISSN

2470-9468

Authors

Nicolai, Christopher J
Wolf, Natalie
Chang, I-Chang
et al.

Publication Date

2020-03-13

DOI

10.1126/sciimmunol.aaz2738

Peer reviewed

HHS Public Access

Author manuscript

Sci Immunol. Author manuscript; available in PMC 2020 September 20.

Published in final edited form as:

Sci Immunol. 2020 March 20; 5(45): . doi:10.1126/sciimmunol.aaz2738.

NK cells mediate clearance of CD8+ T cell–resistant tumors in response to STING agonists

Christopher J. Nicolai[1], **Natalie Wolf**[1], **I-Chang Chang**[1], **Georgia Kirn**[1], **Assaf Marcus**[1], **Chudi O. Ndubaku**[2], **Sarah M. McWhirter**[2], **David H. Raulet**[1,*]

[1]Division of Immunology and Pathogenesis, Department of Molecular and Cell Biology, University of California, Berkeley, Berkeley, CA 94720, USA.

[2]Aduro Biotech, Inc. Berkeley, CA 94710, USA.

Abstract

Several immunotherapy approaches that mobilize $CD8^+$ T cell responses stimulate tumor rejection, and some, such as checkpoint blockade, have been approved for several cancer indications and show impressive increases in patient survival. However, tumors may evade $CD8^+$ T cell recognition via loss of MHC molecules or because they contain few or no neoantigens. Therefore, approaches are needed to combat $CD8^+$ T cell-resistant cancers. STING-activating cyclic dinucleotides (CDN) are a new class of immune-stimulating agents that elicit impressive $CD8^+$ T cell-mediated tumor rejection in preclinical tumor models and are now being tested in clinical trials. Here we demonstrate powerful CDN-induced, natural killer (NK) cell-mediated tumor rejection in numerous tumor models, independent of $CD8^+$ T cells. CDNs enhanced NK cell activation, cytotoxicity, and antitumor effects in part by inducing type I IFN (IFN). IFN acted in part directly on NK cells *in vivo*, and in part indirectly via the induction of IL-15 and IL-15 receptors, which were important for CDN-induced NK activation and tumor control. After *in vivo* administration of CDNs, dendritic cells (DCs) upregulated IL-15Rα in an IFN-dependent manner. Mice lacking the type I IFN receptor specifically on DCs had reduced NK cell activation and tumor control. Therapeutics that activate NK cells, such as CDNs, checkpoint inhibitors, NK cell engagers, and cytokines, may represent next-generation approaches to cancer immunotherapy.

One Sentence Summary:

*corresponding author: raulet@berkeley.edu.

Author contributions: C.J.N., N.W., I.C.C., G.K., and A.M. conducted and analyzed experiments. C.O.N. and S.M.M. provided reagents. C.J.N. and D.H.R. conceived the study, designed and interpreted experiments, and prepared the manuscript. All authors critically read the manuscript.

Competing Interests: C.O.N. and S.M.M. have served as paid employees of Aduro Biotech, are listed as inventors on Aduro Biotech patents and patent applications related to CDNs, and hold stock in Aduro Biotech. D.H.R. is a co-founder of Dragonfly Therapeutics and served or serves on the scientific advisory boards of Dragonfly, Aduro Biotech, Innate Pharma, and Ignite Immunotherapy; he has a financial interest in all four companies and could benefit from commercialization of the results of this research. All other authors declare that they have no competing interests.

Data and Materials Availability: The CDN used in this study, (2'3') RR cyclic di-AMP, was provided under a Material Transfer Agreement between U.C. Berkeley and Aduro Biotech. This material is the property of Aduro Biotech, but CDN compounds with the same structure can be purchased from commercial vendors. This compound is described in a U.S. patent (9,724,408) assigned to Aduro Biotech and the University of California. All $B2m^{-/-}$ cell lines used in this study are available upon request. All data needed to evaluate the conclusions in the paper are available in the main text or the Supplementary Materials.

STING agonists trigger NK cell-mediated clearance of MHC-deficient and MHC-expressing tumors that are resistant to $CD8^+$ T cells.

Introduction

Recent breakthroughs in tumor immunology have provided novel immune-based therapeutics, extending patient lives and in some cases resulting in what appear to be permanent remissions (1, 2). Most immunotherapy protocols aim to augment $CD8^+$ T cell responses by targeting immune inhibitory pathways, leading to greater T cell activation and tumor destruction (3, 4). However, tumors may evade the $CD8^+$ T cell response via selective or complete loss of MHC class I expression (5–7) or because they express few or no neoantigens (8), and may consequently be refractory to $CD8^+$ T cell-dependent therapies. Therefore, knowledge of how the immune system can be mobilized to kill $CD8^+$ T cell-resistant tumors is needed to address these potential escape mechanisms and design next generation immunotherapies.

Natural killer (NK) cells are cytotoxic innate lymphocytes that are important for killing virus-infected cells and tumor cells (9–11). Unlike T cells, which target unique peptide antigens displayed on MHC molecules, NK cells recognize abnormally expressed, stress-induced ligands on unhealthy cells (11–14), and/or cells that have lost MHC class I (15–18). Furthermore, NK cells produce cytokines and chemokines that enhance recruitment and maturation of dendritic cells (DCs) (19, 20), promoting adaptive immune responses. These features enable NK cells to increase adaptive immune responses to tumors as well as directly kill tumors that have escaped T cell responses, making NK cells exciting targets for immunotherapy.

The cGAS-STING pathway is an innate immune sensing pathway that senses cytosolic DNA, resulting in production of type I interferon (IFN) and proinflammatory cytokines and chemokines (21, 22). Upon binding double-stranded DNA, the cGAS enzyme generates the second messenger 2’3’ cyclic GMP-AMP (cGAMP) (21, 23, 24). cGAMP binds and activates the endoplasmic reticulum membrane protein STING (21, 22), triggering recruitment of TBK1 and phosphorylation and activation of IRF3 and NF-κB transcription factors (21).

The cGAS-STING pathway is essential for sensing certain viral and bacterial pathogens (21), but is also activated in tumor cells (25). Moreover, mice lacking functional STING are more susceptible to both transplanted (26, 27) and carcinogen-induced tumors (28). Cytosolic tumor DNA is thought to initiate the response (26, 27) and induces production of cGAMP, which is transferred to other cells to activate STING (27, 29, 30), promoting cytokine production and activation of antitumor responses by both $CD8^+$ T cells (26, 31) and NK cells (27). However, the amounts of cGAMP made or transferred appear to be limiting for inducing a maximally potent antitumor response. Injection of cGAMP or other STING agonists directly into tumors induces a powerful antitumor response leading to tumor rejection in various tumor transplant models of cancer (32–36). Based on these findings, STING agonists are currently being tested in clinical trials.

The antitumor effects of STING agonists have primarily been attributed to $CD8^+$ T cells (32, 35, 37), while their impact on other cells, such as NK cells, remains poorly defined. STING activation potently induces multiple inflammatory mediators, including type I IFNs (22), which play central roles in NK cell biology, including maturation, homeostasis, and activation (38). In this study, we have investigated the role of NK cells in mediating tumor rejection after cyclic dinucleotide (CDN) therapy, independent of the $CD8^+$ T cell response. Our results demonstrate powerful CD8-independent antitumor responses mediated by NK cells that are induced by therapeutic applications of CDNs in numerous cancer models, including both MHC I-deficient and MHC I-sufficient tumor models.

Results

Successful immunotherapy of MHC class I-deficient tumors by CDNs occurs independently of $CD8^+$ T cells.

To examine the $CD8^+$ T cell-independent antitumor effects of intratumoral (i.t.) CDN injection, we employed CRISPR-Cas9 to disrupt *B2m* in multiple tumor cell lines, generating cells with severely diminished levels of cell surface MHC I molecules (Figure 1A and S1). Such tumors have potential clinical relevance in light of evidence that MHC I-deficiency is selected for when T cell responses against tumors are induced, and is common in certain cancers (5–7, 39–41). Tumors were established with a high dose of MHC I-deficient cells injected subcutaneously in syngeneic mice, and treated i.t. once, or in some cases three times, with mixed-linkage (2'3') RR cyclic di-AMP (33) (also known as ADU-S100 and hereafter referred to as "CDN"), or PBS. The dose of CDN used has been shown to be optimal for $CD8^+$ T cell responses (32). CDN injections resulted in regression and severely delayed tumor growth in each of six $B2m^{-/-}$ tumor models tested, representing multiple types of cancer (Figure 1B). Notably, in all but one model there was a significant incidence of long-term remissions as a result of single agent i.t. administration of CDN, with no evidence of renewed tumor growth for the remainder of the study (50–100 days). The impact of CDNs was abrogated in $Sting^{gt/gt}$ mice in both tumor models subsequently tested, demonstrating the role of host STING in the responses (Figure 1C). Depletion of $CD8^+$ T cells using CD8b.2 antibody (Figure S2) did not diminish tumor rejection in either of the two models tested, consistent with the absence of MHC I molecules on the tumor cells (Figure 1D). These data showed that i.t. injections of CDNs trigger potent antitumor effects independently of $CD8^+$ T cells.

CDN-induced rejection of MHC I-deficient tumors depends on NK cells.

To test the role of NK cells, we used anti-NK1.1 antibody to deplete mice of NK cells before tumor implantation and subsequent CDN treatment. NK-depletion (Figure S2) resulted in rapid tumor growth in all five tumor models tested, including MC-38-$B2m^{-/-}$ (colorectal), B16-F10-$B2m^{-/-}$ (melanoma), CT26-$B2m^{-/-}$ (colorectal), C1498-$B2m^{-/-}$ (leukemic), and RMA-$B2m^{-/-}$ (lymphoma) tumor models (Figure 2A). For the RMA-$B2m^{-/-}$ lymphoma line, CDN therapy was also defective in NK-DTA mice, which specifically lack NK cells due to diphtheria toxin expression only in $NKp46^+$ cells (42) (Figure 2B). CDN-induced tumor rejection also occurred in $Rag2^{-/-}$ mice, which lack T and B cells, but was strongly diminished in NK-depleted $Rag2^{-/-}$ mice (Figure 2C), or in $Rag2^{-/-}Il2rg^{-/-}$ mice, which

lack NK cells and other innate lymphoid cells in addition to lacking T and B cells (Figure 2D). Thus, CDNs mobilize powerful NK responses against MHC I-deficient tumors that are quite effective in the absence of T and B cells.

Without NK cells, T cells or B cells, as in *Rag2*$^{-/-}$*Il2rg*$^{-/-}$ mice, CDN injections caused a residual delay in tumor growth (Figure S1B, 2C and 2D). Consistent with previous evidence that STING agonists induce an immediate local hemorrhagic necrosis in tumors, mediated by TNF-α (34), the CDN-induced delay in the growth of RMA-*B2m*$^{-/-}$ tumors was eliminated when TNF-α was neutralized in *Rag2*$^{-/-}$*Il2rg*$^{-/-}$ mice (Figure S1B). Notably, the delay in tumor growth in *Rag2*$^{-/-}$*Il2rg*$^{-/-}$ mice was transient and none of the mice survived, showing that robust antitumor effects depended on lymphocytes.

Many tumor cells express high MHC I but are nevertheless sensitive to NK cells due to high expression of NK-activating ligands (18, 43). An important question was whether CDN-induced, NK-mediated, antitumor effects would be effective against MHC I-high tumor cells that are NK-sensitive. To address this question, we employed the WT (*B2m*$^{+/+}$) MC-38 line, which is MHC I-high (Figure 1A), but which NK cells kill effectively *in vitro* due, at least in part, to the expression of NKG2D ligands by these tumor cells (43). Remarkably, in *Rag2*$^{-/-}$ mice, which lack all T cells and B cells, CDN treatment was effective in delaying growth of MC-38 tumors and even resulted in a few long-term survivors (Figure 2E). NK depletion resulted in rapid tumor growth and eliminated any long-term survivors. Thus, NK cells can reject MHC I^{+} MC-38 tumor cells after CDN injections, even in the complete absence of T cells. We conclude that CDN-induced NK responses are effective not only against MHC I-deficient tumors but also against tumors that are NK sensitive due, for example, to expression of NK-activating ligands.

NK cells are activated by i.t. CDN injections and accumulate within tumors.

To address the impact of CDN treatments on NK cells, we examined markers of NK cell activation among tumor-infiltrating, lymph node, and splenic NK cells one day after treatment, with no additional stimulation *ex vivo*. Compared to NK cells within PBS-treated tumors, NK cells within CDN-treated tumors had increased levels of IFN-γ, the degranulation marker CD107a, granzyme B, and Sca-1 (Figure 3A and S3), demonstrating an increased degree of NK activation. Furthermore, NK cells accumulated among CD45^{+} cells within CDN-treated tumors (Figure 3B). The relative increase of NK cells within tumors coincided with an increase in Ki67 expression (Figure 3B and S4), suggesting that CDNs promote NK cell proliferation in addition to activation.

CDN treatment also caused NK activation in the tumor-draining lymph node and even in the spleen (Figure 3A), suggesting that i.t. injection of CDNs resulted in systemic NK activation. Consistent with systemic activation, we found that splenocytes harvested from tumor-bearing CDN-treated mice, but not PBS-treated control mice, exhibited detectable cytotoxicity against RMA-*B2m*$^{-/-}$ tumor cells *ex vivo* (Figure 3C). Depleting NK cells after harvest abolished the killing.

Based on these observations, we tested whether systemic NK cell activation induced by CDN administered locally in one tumor would also trigger antitumor responses in an

untreated distal tumor. We established C1498-*B2m*$^{-/-}$ tumors on both flanks of *Rag2*$^{-/-}$ mice and treated one tumor with PBS or CDN. As expected based on the results in Figure 1B, i.t. CDN treatment caused substantial tumor regression in the injected tumor (Figure 3D). Notably, there was also a significant growth delay in the untreated distal (contralateral) tumor compared to PBS, showing that i.t. CDN treatments induce systemic antitumor effects, independent of T and B cells. Similar results were obtained with a separate tumor model, B16-F10-*B2m*$^{-/-}$, in T cell-depleted WT mice (Figure S5). When mice with C1498-*B2m*$^{-/-}$ tumors were depleted of NK cells the antitumor effects at both the treated and distal tumor were severely abrogated. As these mice lack all T cells and B cells, the results demonstrate that the systemic, CDN-induced effects were mediated by NK cells independently of T cells (Fig 3D). In conclusion, i.t. CDN treatment induced NK activation within tumors and to some extent systemically, enhanced *ex vivo* NK killing capacity, and exerted antitumor effects on a distant tumor.

NK cell activation and tumor rejection are dependent on type I interferon acting on host cells.

Consistent with the known role of STING activation in type I IFN production (22), we observed a marked increase in *Ifnb1* transcripts within tumors 24 hours after CDN treatment compared to PBS-treated controls (Figure 4A). Serum of CDN-treated mice also contained high levels of IFN-β shortly after treatment (Figure 4B). These data are consistent with a recent study showing low but detectable circulating IFN-β in patients treated with CDNs combined with anti-PD-1 (44). The systemic anti-tumor effects reported in Figure 3 may be explained, at least in part, by the induction of significant levels of systemic IFN-β by local CDN treatments. NK cell activation was strongly dependent on type I IFN as CDN-treated *Ifnar1*$^{-/-}$ mice, which lack functional type I IFN receptors, did not display increases in IFN-γ, CD107a, granzyme B, or Sca-1 in response to CDNs compared to WT controls (Figure 4C and S6). Similar results were obtained in the tumor-draining lymph nodes and spleens of WT mice injected with IFNAR1-blocking antibodies (Figure S7A and S7B). Furthermore, splenocytes from CDN-treated *Ifnar1*$^{-/-}$ mice, or WT mice given IFNAR1-blocking antibodies, were unable to kill RMA-*B2m*$^{-/-}$ tumor cells *ex vivo,* unlike splenocytes from CDN-treated WT mice (Figure 4D and S7C). Therefore, type I IFN action is essential for NK cell activation and deployment of effector functions after CDN injections.

In terms of tumor rejection, both MHC I-deficient tumor cell lines tested, RMA-*B2m*$^{-/-}$ and MC-38-*B2m*$^{-/-}$, were refractory to CDN therapy in *Ifnar1*$^{-/-}$ mice (Figure 4E). Knocking out *Ifnar1* in RMA-*B2m*$^{-/-}$ tumor cells had no effect on tumor rejection (Figure S7D), indicating that type I IFN action on host cells, rather than tumor cells, is necessary for the response. Importantly, IFNAR1 neutralization also abrogated the antitumor effects of CDN therapy for RMA-*B2m*$^{-/-}$ tumors (Figure S7E), suggesting that acute effects of CDN-induced type I IFN, rather than developmental or homeostatic effects, are key to the antitumor response. NK depletion combined with IFNAR1 blockade had no greater effect than either treatment alone in *Rag2*$^{-/-}$ mice (Figure 4F), supporting the conclusion that the NK-mediated antitumor activity is strongly dependent on type I IFN.

Type I IFN acts directly on NK cells to mediate the antitumor response.

We initially employed bone marrow chimeras between WT and *Ifnar1*$^{-/-}$ mice to address the cell types on which type I IFN acts to mediate NK-dependent antitumor responses. The chimeric mice, which showed near complete chimerism (Figure S8), were implanted with RMA-*B2m*$^{-/-}$ tumor cells, and the established tumors were subjected to i.t. CDN therapy. Tumor rejection in *Ifnar1*$^{-/-}$ → *Ifnar1*$^{-/-}$ and *Ifnar1*$^{-/-}$ → WT chimeras was largely impaired compared to control chimeras, whereas WT → *Ifnar1*$^{-/-}$ chimeras behaved like WT → WT controls. These data argue that the action of type I IFN on hematopoietic cells is necessary and mostly sufficient for tumor rejection (Figure 4G). In this and another experiment, there were hints that type I IFN acting on radioresistant cells may play a minor role in the rejection response, such as the slight delay in tumor growth in *Ifnar1*$^{-/-}$ → WT chimeras compared to *Ifnar1*$^{-/-}$ → *Ifnar1*$^{-/-}$ chimeras in Figure 4G (p=0.036).

To examine if direct effects of type I IFN on NK cells were important for CDN-induced antitumor effects we employed *Ncr1-iCre, Ifnar1*$^{fl/fl}$ mice, in which *Ifnar1* expression is defective only in NK cells (Figure S9). *Ifnar1* deletion in NK cells was highly efficient (Figure S9). *In vivo*, *Ncr1-iCre, Ifnar1*$^{fl/fl}$ mice were unable to control tumor growth after CDN therapy and had reduced overall survival, indicating the importance of direct type I IFN action on NK cells for tumor rejection (Figure 5A). However, the defect in tumor control was not as substantial as in NK-depleted mice (Figure 5A) or as in *Ifnar1*$^{-/-}$ mice (Figure 5B), suggesting that type I IFN boosts NK-mediated tumor rejection in part by acting indirectly on non-NK cells. Furthermore, NK cells in the tumor-draining lymph nodes of CDN-treated *Ncr1-iCre, Ifnar1*$^{fl/fl}$ mice had decreased levels of IFN-γ, granzyme B, Sca-1, and CD107a (Figure 5C and S10), though they were not reduced to the control levels observed in *Ifnar1*$^{fl/fl}$ mice (no Cre) treated with PBS. We also observed that *Ifnar1* deletion specifically in NK cells resulted in a sharp reduction in CDN-induced cytotoxicity of splenocytes against RMA-*B2m*$^{-/-}$ tumor cells, though a very small amount of cytotoxicity may remain (Figure 5B). These data show that type I IFN acts directly on NK cells, but likely also acts on another cell type(s) to indirectly enhance NK cell activation.

CDN-induced type I IFN acts on DCs to boost NK cell activation, and enhance antitumor effects.

Type I IFN is a key modulator of dendritic cell (DC) function, promoting maturation and immune stimulatory functions (45, 46). We therefore hypothesized that CDN-induced type I IFN was acting in part on DCs, promoting NK cell effector function and enhanced tumor control. To determine if type I IFN-dependent DC activation was important for NK cell activation we employed *Cd11c-Cre, Ifnar1*$^{fl/fl}$ mice, in which *Ifnar1* undergoes deletion specifically in CD11c^{+} cells such as DCs (Figure S11). IFNAR1 expression was lost in most, but not all, CD11c^{+} MHC II^{+} cells in these mice (Figure S11). *Cd11c-Cre, Ifnar1*$^{fl/fl}$ mice exhibited a partial defect in tumor rejection compared to *Ifnar1*$^{fl/fl}$ (no Cre) control mice (Figure 6A), indicating a role for type I IFN acting on DCs. The defect was modest, however, in comparison to the defect in *Ifnar1*$^{-/-}$ mice or NK-depleted mice (Figure 6A), consistent with type I IFN action on other cells, such as NK cells as shown in Figure 5C and 5D. Relative to NK cells in *Ifnar1*$^{fl/fl}$ (no Cre) control mice, NK cells in the tumor-draining lymph nodes of CDN-treated *Cd11c-Cre, Ifnar1*$^{fl/fl}$ mice had lower levels of IFN-γ,

Granzyme B, and Sca-1 (Figure 6B and S12), indicating that type I IFN signaling on DCs is required for full NK cell activation. Again, however, the defect was only partial compared to PBS-treated control mice (Figure 6B). Degranulation (CD107a) levels were similar between the two groups, suggesting that for degranulation the direct action of type I IFN on NK cells may be more important than the indirect effects mediated by DCs. Splenocytes from CDN-treated *Cd11c-Cre, Ifnar1*$^{fl/fl}$ mice also showed a small but reproducible reduction in *ex vivo* cytotoxicity against RMA-*B2m*$^{-/-}$ tumor cells (p=0.02) (Figure 6C). Together, these data indicate that in CDN-treated tumors, type I IFN acts indirectly on DCs and directly on NK cells in promoting both NK cell activation and the rejection of tumors by NK cells.

IL-15 is induced by CDN injections, dependent on type I IFN, and is important for the antitumor response.

To address how type I IFN acts on DCs to enhance NK cell activation, we determined the impact of type I IFN on DC IL-15-IL-15Rα expression after CDN treatments. Unlike many cytokines, IL-15 is trans-presented to cells: it associates with the IL-15Rα chain during synthesis and the IL-15-IL-15Rα complex is presented to responding cells (47), where it binds the IL-2/15Rβ chain leading to signaling by the common γ chain, γC. IL-15 signaling is especially important for NK cell biology as it enhances effector functions and promotes survival (48).

CDN-treated tumors had elevated levels of *Il15* and *Il15ra* transcripts relative to PBS-treated controls 24 hours after treatment (Figure 7A). In parallel, cell surface IL-15Rα expression was elevated in numerous cell types in the tumor-draining lymph node and spleen, including DCs, macrophages, monocytes, neutrophils, and interestingly, NK cells (Figure 7B and S13). IFNAR1 blockade during CDN treatment inhibited the induction of *Il15* and *Il15ra* transcripts in tumors, and cell surface IL-15Rα expression on the aforementioned cell types (Figures 7A, 7B, S13). These data indicate that CDN treatment, mainly via the action of type I IFNs, induces IL-15/IL-15Rα expression on numerous cell types in the tumor microenvironment and systemically.

When IL-15 was neutralized during CDN treatment, NK cells in the tumor-draining lymph nodes had significantly reduced IFN-γ, CD107a, granzyme B, and Sca-1 (Figure 7C and S14). In addition, neutralizing IL-15 caused a small but reproducible reduction in *ex vivo* cellular cytotoxicity (p=0.03) (Figure 7D). Finally, CDN-induced control of RMA-*B2m*$^{-/-}$ tumors was markedly diminished in mice given IL-15 neutralizing antibodies (Figure 7E). Overall, the data suggest that CDNs induce IL-15 production and presentation, potentially by multiple cell types, in a type I IFN-dependent manner. The IL-15 then acts to boost NK cell effector function and tumor killing capacity, leading to greater tumor control *in vivo*.

Discussion

The immunotherapeutic potential of NK cells for cancer, including solid cancers, has not been fully established. Our data demonstrate therapy-induced NK-dependent long-term remissions of several types of transplanted MHC I-deficient, CD8^{+} T cell-resistant, solid tumors. Importantly, the impressive impact of NK-dependent antitumor responses was not limited to MHC I-deficient tumors, but also occurred in MHC I-high MC-38 tumors in

Rag2$^{-/-}$ mice, with some mice exhibiting long-term remissions. Like many tumor lines, MC-38 cells express abundant NKG2D ligands and these cells are killed efficiently by NK cells *in vitro* (43), despite the high MHC I expression. It is likely that the key attribute predicting favorable NK-dependent effects induced by CDNs or other NK-mobilizing therapeutics is not solely MHC I deficiency but rather the overall sensitivity of the cells to NK cell killing, which reflects a balance of activating and inhibitory interactions (18).

Considering that most tumor cells express NKG2D ligands (49) or other ligands that activate NK cells (14), and are sensitive to NK killing *in vitro*, therapies that amplify NK cell activity have the potential to show efficacy in a broad variety of cancers, including many that are resistant to destruction by T cells. We propose that such therapies will complement therapies that mobilize T cell responses, including checkpoint therapies, by eliminating variants with antigen presentation defects. Therapeutic mobilization of NK cells may be especially important for tumors that lack strong T cell epitopes or have lost MHC expression, as well as for combining with therapeutic antibodies that mediate antibody-dependent cellular cytotoxicity mediated by NK cells.

STING-agonists have shown dramatic efficacy in preclinical cancer models and are currently being tested in clinical trials. Most studies have focused on T cell-mediated responses induced by CDNs (32, 33, 35). In the present study we demonstrated that intratumoral injection of CDNs triggered potent, NK-dependent, and CD8-independent rejection of several different NK-sensitive tumors originating from multiple tissue types. Notably, CDN injection triggered complete tumor rejection and long-term survival in a portion of the mice in most of the models tested.

Some of our studies utilized *B2m*$^{-/-}$ tumor cells, which lack MHC I, and are therefore more sensitive to NK cells because they fail to engage inhibitory KIR (or Ly49 in mice) (16, 17). These models are potentially clinically relevant as many human tumors exhibit at least a partial loss of surface MHC I (5–7). Furthermore, resistance to checkpoint blockade correlates with absence of tumor MHC I expression, with *B2M* mutations found among the non-responding patient tumors (39–41). Other cancers, such as classical Hodgkin's lymphoma, generally have very low MHC I. The efficacy of PD-1 blockade in Hodgkin's lymphoma (6) may possibly be due to the activity of NK cells, given that NK cells express functional PD-1 in mouse tumor models (50).

Our results demonstrate that the CDN-induced, NK-mediated antitumor effects were dependent on type I IFN. A hallmark of STING activation is production of type I IFN and many cell types, including both hematopoietic and nonhematopoietic cells, produce it in response to STING activation in tumors, including DCs, macrophages, monocytes, and endothelial cells. It has been shown that cells in each of these compartments can contribute to the antitumor effects of intratumoral CDN injection (32, 34, 35, 51). Type I IFN enhances T cell responses (46) and is important for cancer immunosurveillance and the efficacy of cancer immunotherapies (38, 52, 53). Type I IFN is also important for NK cell biology (38) and NK cells from *Ifnar1*$^{-/-}$ mice have greatly reduced cytotoxicity against tumor cell lines *in vitro* (38). Less clear is how type I IFN exerts its effects on NK cells, with reports of both direct and indirect action. Consistent with direct action, mice lacking type I IFN signaling

specifically in NK cells had reduced *in vitro* cytotoxicity against tumor cell lines (54). However, that study failed to find a survival difference between *Ncr1-iCre, Ifnar1*$^{fl/fl}$ and *Ifnar1*$^{fl/fl}$ control mice after exposure to oncogenic Abelson murine leukemia virus, leaving it unclear whether type I IFN acts directly on NK cells in the antitumor response.

Other reports have highlighted the importance of indirect action of type I IFN on NK cells, particularly cells of the myeloid lineage. DCs regulate NK cells both through direct interactions and the release of cytokines, such as IL-12, IL-15, and IL-18 (55). IL-15 is especially important for NK cell survival and homeostasis, and is known to promote NK cell proliferation and effector activity (47, 56). Mice lacking *Il15ra* in either LysM- or CD11c-expressing cells exhibited significant defects in NK cell homeostasis and activation (57). Type I IFN induces IL-15 production and presentation by DCs (55, 58) and it has been observed that IL-15 trans-presenting-DCs are required for type I IFN-dependent “priming” of NK cells *in vivo* by TLR agonists or infections for enhanced *ex vivo* stimulation assays (58).

While informative, these studies conflicted in how type I IFN stimulates NK cells, and the role of type I IFN for NK cell-mediated tumor control *in vivo* remained unclear. Our findings provide clarity by indicating that both direct action of type I IFN and indirect action, via IL-15, are important for maximum NK cell antitumor activity *in vivo*. Our studies suggest that DCs are significant contributors to indirect NK activation by type I IFN *in vivo*, but do not rule out a role for other myeloid cell populations. In fact, we observed that other cell types upregulated IL-15R after CDN treatments, including monocytes, macrophages, and even NK cells, suggesting that these other cell types may play some role in amplifying NK activity. We cannot test definitively whether the response depends on IL-15 from DCs with available tools, because studies show that mice lacking IL-15 expression specifically in DCs (as well as those lacking IL-15 expression in macrophages) exhibit steady-state defects in NK cell numbers and functionality (57), making it impossible to attribute any phenotypes we might observe to events occurring after establishing tumors and injecting CDNs. It has also been reported that tumors from patients with colorectal cancer have mutations in IL-15 and other cytokines and that this correlates with higher risk of tumor recurrence and decreased survival, suggesting that tumors may also be relevant sources of NK-activating cytokines (59). Our study found that type I IFN action on host cells, and not the tumor, was crucial for the antitumor effect in our model, but it remains possible that IFN induces IL-15 production by tumor cells in other cancers or models. Furthermore, we cannot rule out the importance of other CDN-induced, IFN-independent tumor-derived molecules. Finally, we note that in addition to effects of CDNs on IL-15 (via IFN), CDNs are known to induce numerous other cytokines, chemokines and cell surface receptors, and it is highly likely that some of those other induced molecules also play important roles in the antitumor NK response.

CDN-treatment led to systemic activation of NK cells and delayed the growth of distal tumors. Intratumoral injections of CDN led to increased levels of IFN-β in the serum and it is likely that the systemic type I IFN response promoted the systemic NK cell activation and antitumor effects. There are, however, other potential mechanisms of systemic NK cell activation that may play some role. When very high doses of CDNs are injected in mice with

two tumors, some leakage from the injected tumor occurs and low amounts of CDNs can be detected in distal tumors (32). While we used much lower doses of CDN than in that study, it remains possible that CDN leakage from the tumors into the circulation contributed to the systemic activation we observed. The possibility that large numbers of NK cells that were initially activated locally near the tumor recirculated to the spleen and to distal tumors appears less likely given that such a large percentage of splenic NK cells were activated shortly after local CDN administration. Regardless of the exact mechanism, our data makes clear that i.t. CDN treatment alone is capable of promoting antitumor effects on distal tumors independently of T cells.

Cancer immunotherapy, especially checkpoint blockade, has led to major improvements in cancer treatment (1, 2), and while substantial numbers of long-term remissions have been achieved in several cancers, many patients do not respond. Combining checkpoint therapy with CDN therapy may be beneficial not only because CDNs amplify T cell responses (32, 35), but because tumor cells in patients treated with checkpoint inhibitors are sometimes selected for loss of MHC I (39–41), and CDN-activated NK cells may eliminate those cells. Furthermore, NK cells in tumors express checkpoint receptors such as PD-1 and TIGIT (50, 60), suggesting that checkpoint therapy could enhance the function of CDN-activated NK cells. Combinations of CDNs with NK-activating inflammatory cytokines such as IL-15, IL-12 and IL-18 may also provide added benefit (61, 62). Finally, blocking endogenous interactions that lead to NK cell desensitization (63, 64) or providing CDNs in combination with antibodies that mediate NK-dependent antibody-dependent cellular cytotoxicity of cancer cells may also be impactful.

In conclusion, our results show that $CD8^+$ T cell-resistant tumors can be effectively treated using CDNs. The antitumor effects were mediated by NK cells and dependent on type I IFN, which boosts NK cell antitumor responses *in vivo.* Mechanistically, type I IFN boosts NK cell responses by both direct action and indirect action via DCs, which induce IL-15 to further promote NK activation and tumor destruction (Figure 7F). These findings support the view that NK cells could be a cornerstone of next-generation cancer immunotherapies.

Materials and Methods

Study Design

The objectives of this work were to examine the mechanisms of NK cell-mediated antitumor effects after i.t. CDN treatment of MHC I-deficient and MHC I-expressing tumors. For our studies tumors were established subcutaneously in mice, PBS or CDNs were injected intratumorally, and tumor growth, overall survival, and NK cell activation status were recorded. Male and female mice were equally used, and experimental groups/treatments were randomized among mice in the same cage when possible. Generally, experimental groups consisted of at least 5–6 mice, but in some experiments up to 12 were used. We did not use a power analysis to calculate sample size and did not exclude data. All experiments were done at least twice, and in some cases, experiments were pooled. The investigators were not blinded.

Mouse strains

Mice were maintained at the University of California, Berkeley. C57BL/6J, CD45.1-congenic (B6.SJL-*Ptprc*^{a} *Pepc*^{b}/BoyJ), *Rag2*$^{-/-}$, *Rag2*$^{-/-}$ *Il2rg*$^{-/-}$, *Ifnar1*$^{-/-}$ (all on the B6 background), and BALB/cJ mice were purchased from the Jackson Laboratory. *Ncr1*^{iCre} and *Sting*$^{gt/gt}$ mice on the B6 background were generous gifts from Eric Vivier and Russell Vance, respectively. NK-DTA mice were generated by breeding *Ncr1*^{iCre} mice to B6-*Rosa26*$^{LSL\text{-}DTA}$ mice (Jackson Laboratories). *Ncr1*$^{iCre/+}$, *Ifnar1*$^{fl/fl}$ and *CD11c-Cre, Ifnar1*$^{fl/fl}$ mice, all on the B6 background, were generated by breeding *Ncr1*^{iCre} and *CD11c (Itgax)-Cre-eGFP* (Jackson Laboratories) mice to *Ifnar1*$^{fl/fl}$ mice (Jackson Laboratories). All mice used were aged 8–30 weeks. All experiments were approved by the UC Berkeley Animal Care and Use Committee.

Cell lines and culture conditions

RMA (obtained from Michael Bevan, who received it from Dr. K. Karre, Karolinska Institute, Stockholm, Sweden), CT26 (obtained from Aduro Biotech), 4T1 (obtained from Dr. Robert Weinberg), and C1498 (purchased from ATCC) were cultured in RPMI 1640 (ThermoFisher). B16-F10 (obtained from the UC Berkeley Cell Culture Facility) and MC-38 (obtained from Dr. James Allison) were cultured in DMEM (ThermoFisher). In all cases media contained 5% FBS (Omega Scientific), 0.2 mg/ml glutamine (Sigma-Aldrich), 100 U/ml penicillin (Thermo Fisher Scientific), 100 μg/ml streptomycin (Thermo Fisher Scientific), 10 μg/ml gentamycin sulfate (Lonza), 50 μM β-mercaptoethanol (EMD Biosciences), and 20 mM HEPES (Thermo Fisher Scientific), and the cells were cultured in 5% CO_2. *B2m*$^{-/-}$ cell lines were generated using CRISPR-Cas9 (described below). All cells tested negative for mycoplasma contamination.

Generation of cell lines using CRISPR-Cas9

Plasmids containing Cas9 and *B2m*-targeting guide sequence were generated previously (62). The *Ifnar1*-targeting CRISPR-Cas9 plasmid was generated by cloning the guide sequence (GCTGGTGGCCGGGGCGCCTT) into PX330 (Addgene) following the recommended protocol. To generate knockout cell lines, plasmids were transiently transfected using either Lipofectamine 2000 (ThermoFisher) (CT26, 4T1, B16-F10, and MC-38) or by nucleofection (RMA and C1498) (Kit T, Lonza). One week later, MHC I or IFNAR1-deficient cells were sorted using a FACS Aria cell sorter. For B16-F10, cells were incubated with 100 ng/ml IFN-β (Biolegend) overnight before sorting in order to easily distinguish MHC I^{+} and MHC I^{-} cells.

In vivo tumor growth experiments

Cells were washed and resuspended in PBS (ThermoFisher) and 100 μl containing 4×10^{6} cells were injected subcutaneously. Tumor growth was measured using calipers and tumor volume estimated using the ellipsoid formula: $V = (\pi/6)ABC$. In some experiments, mice were NK-depleted by intraperitoneal (i.p.) injection of 250 μg anti-NK1.1 (clone PK136, purified in our laboratory) or 100 μl anti-asialo-GM1 (Biolegend) for C57BL/6J and BALB/c mice, respectively. Mice were CD8- and CD4-depleted by i.p. injection of 250 μg anti-CD8b.2 (clone 53.5.8, Leinco) or 250 μg anti-CD4 (clone GK1.5, Leinco), respectively.

Whole rat Ig (Jackson Immunoresearch) was used as a control. Depleting or control antibodies were injected 2 days and 1 day before tumor inoculation and continued weekly thereafter. Depletions were confirmed by flow cytometry. 5 days after tumor inoculation, when tumors were ~50–150 mm^3, mice were injected i.t. with PBS or 1× 50 μg c-di-AMP (RMA-*B2m*$^{-/-}$, B16-F10-*B2m*$^{-/-}$, C1498-*B2m*$^{-/-}$, MC38-*B2m*$^{-/-}$) or 3 × 25 μg c-di-AMP (CT26-*B2m*$^{-/-}$, 4T1-*B2m*$^{-/-}$) in a total volume of 100 μl (PBS). In some experiments, mice received 500 μg anti-IFNAR1 (clone MAR1–5A3, Leinco), 200 μg anti-TNF-α (clone TN3–19.12, Leinco), or control rat IgG i.p. on day −1, day 0, and again on days 1 and 4. In some experiments, mice received 5 μg anti-IL-15/15R (clone GRW15PLZ, Thermo Fisher Scientific) or control rat IgG i.p. on day −1, once again i.t. mixed with CDN on day 0, and again i.p. on days 1 and 2.

Flow Cytometry

Single cell suspensions of spleens and lymph nodes were generated by passing cells through a 40 μm filter. Red blood cells were removed from spleens using ACK lysing buffer (made in our laboratory). Tumors were chopped with a razor blade and dissociated in a gentleMACS Dissociator (Miltenyi) before passage through an 80 μm filter. For assessing NK activation, cell suspensions were incubated for 4 hours in medium containing brefeldin A (Biolegend), monensin (Biolegend) and anti-CD107a antibodies before surface and intracellular staining. LIVE/DEAD stain (ThermoFisher) was used to exclude dead cells. FcγRII/III receptors were blocked with 2.4G2 hybridoma supernatant (prepared in the lab). Staining with fluorochrome- or biotin-conjugated antibodies occurred at 4°C for 30 min in FACS buffer (2.5% FBS and 0.02% sodium azide in PBS). When necessary, fluorochrome-conjugated streptavidin was added. For intracellular staining, cells were fixed and permeabilized using Cytofix/Cytoperm buffer (BD Biosciences) and stained with fluorochrome-conjugated antibodies for 30 min at 4°C in Perm/Wash buffer (BD Biosciences). Flow cytometry was performed using an LSR Fortessa, or X20 (BD Biosciences). Data analyzed with FlowJo (Tree Star).

Antibodies

For flow cytometry we used the following antibodies: Biolegend: anti-CD45 (30-F11), anti-CD45.1 (A20), anti-CD45.2 (104), anti-CD3ε (145–2C11), anti-CD4 (GK1.5), anti-CD11b (M1/70), anti-CD11c (N418), anti-CD19 (6D5), anti-F4/80 (BM8), anti-Ly6C (HK1.4), anti-Ly6G (1A8), anti-NKp46 (29A1.4), anti-NK1.1 (PK136), anti-Sca-1 (D7), anti-Ter119 (TER-119), anti-Ki67 (SolA15), anti-CD107a (1D4B), anti-I-A/I-E (M5/114.15.2), anti-IFN-γ (XMG1.2), and anti-IFNAR1 (MAR1–5A3); BD Biosciences: anti-H-2K^b (AF6–88.5) and anti-granzyme B (GB11); R&D Systems: anti-IL-15Rα (BAF551).

Ex *vivo* cytotoxicity assay

Cytotoxicity by splenocytes was assessed with a standard 4-hour ^{51}Cr-release assay. ~24 hours after CDN or PBS treatment of tumors, spleens were harvested and treated with ACK lysing buffer. Pooled splenocytes from 4–6 mice were employed as effector cells. Triplicate samples of 10^4 ^{51}Cr-labeled RMA-*B2m*$^{-/-}$ cells per 96-well V-bottom plate well were incubated with splenocytes at the indicated E:T ratios for 4 hrs before determining the percent ^{51}Cr release in the supernatant. % specific lysis = 100 x (experimental - spontaneous

release$_{Avg}$)/(maximum release$_{Avg}$ - spontaneous release$_{Avg}$), where maximum release was release with addition of Triton X-100 (final concentration 2.5%).

Where shown, pooled splenocytes were NK-depleted by incubating on ice for 30 min with anti-NKp46-biotin (Biolegend) and anti-NK1.1-biotin (Biolegend) followed by 20 min incubation with streptavidin magnetic beads (Biolegend), and magnetic removal of bead-bound cells. Depletion (>95%) was confirmed by flow cytometry.

RNA isolation, reverse transcription, and qPCR

Tumors were harvested and dissociated using the gentleMACS dissociator (Miltenyi), and total RNA was isolated using the RNeasy Mini Kit (Qiagen) and treated with DNase I (Qiagen). cDNA was generated using the iScript reverse transcription kit (BioRad). Quantitative real-time PCR was done using SsoFast EvaGreen Supermix (BioRad) with 25 ng of cDNA per reaction in a CFX96 Thermocycler (BioRad). *Gapdh* and *Ubc* were used as references.

Primer sequences: *Gapdh* F: TGTGTCCGTCGTGGATCTGA, R: TTGCTGTTGAAGTCGCAGGAG; *Ubc* F: GCCCAGTGTTACCACCAAGA, R: CCCATCACACCCAAGAACAA; *Ifnb1* F: ATGAACTCCACCAGCAGACAG, R: ACCACCATCCAGGCGTAGC; *Il15* F: GTGACTTTCATCCCAGTTGC, R: TTCCTTGCAGCCAGATTCTG; *Il15ra* F: CCCACAGTTCCAAAATGACGA, R: GCTGCCTTGATTTGATGTACCAG.

ELISA

Tumors of ~100 mm^3 were injected with PBS or 50 μg CDN. 6 hours later serum was harvested and IFN-β was quantified by ELISA (Biolegend) following the manufacturer's instructions.

Bone marrow chimeras

Recipient mice were irradiated with 10 Gy (5 Gy + 5 Gy on consecutive days) followed by intravenous injection of 10^7 donor bone marrow cells suspended in 100 μl PBS. WT mice were B6-CD45.1 and the *Ifnar1*$^{-/-}$ donors were on the B6 background (CD45.2). After 8 weeks, chimerism was assessed by staining blood cells for CD45.1 and CD45.2 expression and analyzing by flow cytometry, followed by use of the mice in experiments.

Statistics

Statistics were performed using Prism (GraphPad). For tumor growth and survival, two-way ANOVA and Log-rank (Mantel-Cox) tests were used. For NK activation and qPCR, unpaired two-tailed students T tests or one-way ANOVA followed by Tukey's multiple comparisons tests were used when data fit a Normal distribution. For nonparametric data, the Kruskal-Wallis test with Dunn's multiple comparisons was used. Two-way ANOVA was used for cytotoxicity and in some instances the areas under the curves were compared using paired two-tailed Student's T tests. Significance is indicated as: *P < 0.05; **P<0.01; ***P < 0.001; ****P<0.0001.

Supplementary Material

Refer to Web version on PubMed Central for supplementary material.

Acknowledgements:

We thank L. Zhang and E. Seidel for assistance, the UC Berkeley flow core and M. Ardolino for flow cytometry support and training, A. Tubbs for graphic expertise and members of the Raulet Lab and Aduro Biotech for scientific discussions.

Funding: This research was supported by grant 045535 from the UC Berkeley Immunotherapy and Vaccine Research Initiative supported by Aduro Biotech, and NIH grant R01-AI113041 to D.H.R. C.J.N. was supported by an NIH predoctoral fellowship, F31CA228381. The content is solely the responsibility of the authors and does not necessarily represent the official views of the National Institutes of Health.

References and Notes:

1. Sharma P, Allison JP, The future of immune checkpoint therapy. Science 348, 56–61 (2015). [PubMed: 25838373]
2. Ribas A, Wolchok JD, Cancer immunotherapy using checkpoint blockade. Science 359, 1350–1355 (2018). [PubMed: 29567705]
3. Hirano F, Kaneko K, Tamura H, Dong H, Wang S, Ichikawa M, Rietz C, Flies DB, Lau JS, Zhu G, Tamada K, Chen L, Blockade of B7-H1 and PD-1 by monoclonal antibodies potentiates cancer therapeutic immunity. Cancer Res 65, 1089–1096 (2005). [PubMed: 15705911]
4. Leach DR, Krummel MF, Allison JP, Enhancement of antitumor immunity by CTLA-4 blockade. Science 271, 1734–1736 (1996). [PubMed: 8596936]
5. McGranahan N, Rosenthal R, Hiley CT, Rowan AJ, Watkins TBK, Wilson GA, Birkbak NJ, Veeriah S, Van Loo P, Herrero J, Swanton C, Consortium TR, Allele-Specific HLA Loss and Immune Escape in Lung Cancer Evolution. Cell 171, 1259–1271 e1211 (2017). [PubMed: 29107330]
6. Roemer MG, Advani RH, Redd RA, Pinkus GS, Natkunam Y, Ligon AH, Connelly CF, Pak CJ, Carey CD, Daadi SE, Chapuy B, de Jong D, Hoppe RT, Neuberg DS, Shipp MA, Rodig SJ, Classical Hodgkin Lymphoma with Reduced beta2M/MHC Class I Expression Is Associated with Inferior Outcome Independent of 9p24.1 Status. Cancer Immunol Res 4, 910–916 (2016). [PubMed: 27737878]
7. Garrido F, Aptsiauri N, Doorduijn EM, Garcia Lora AM, van Hall T, The urgent need to recover MHC class I in cancers for effective immunotherapy. Current opinion in immunology 39, 44–51 (2016). [PubMed: 26796069]
8. Alexandrov LB, Stratton MR, Mutational signatures: the patterns of somatic mutations hidden in cancer genomes. Curr Opin Genet Dev 24, 52–60 (2014). [PubMed: 24657537]
9. Vivier E, Raulet DH, Moretta A, Caligiuri MA, Zitvogel L, Lanier LL, Yokoyama WM, Ugolini S, Innate or adaptive immunity? The example of natural killer cells. Science 331, 44–49 (2011). [PubMed: 21212348]
10. Marcus A, Gowen BG, Thompson TW, Iannello A, Ardolino M, Deng W, Wang L, Shifrin N, Raulet DH, Recognition of tumors by the innate immune system and natural killer cells. Adv Immunol 122, 91–128 (2014). [PubMed: 24507156]
11. Cerwenka A, Lanier LL, Natural killer cells, viruses and cancer. Nature Rev Immunol 1, 41–49. (2001). [PubMed: 11905813]
12. Raulet DH, Guerra N, Oncogenic stress sensed by the immune system: role of natural killer cell receptors. Nat Rev Immunol 9, 568–580 (2009). [PubMed: 19629084]
13. Raulet DH, Gasser S, Gowen BG, Deng W, Jung H, Regulation of ligands for the NKG2D activating receptor. Annu Rev Immunol 31, 413–441 (2013). [PubMed: 23298206]
14. Moretta A, Bottino C, Vitale M, Pende D, Cantoni C, Mingari MC, Biassoni R, Moretta L, Activating receptors and coreceptors involved in human natural killer cell-mediated cytolysis. Annu Rev Immunol 19, 197–223 (2001). [PubMed: 11244035]

15. Karre K, Ljunggren HG, Piontek G, Kiessling R, Selective rejection of H-2-deficient lymphoma variants suggests alternative immune defence strategy. Nature 319, 675–678 (1986). [PubMed: 3951539]

16. Karlhofer FM, Ribaudo RK, Yokoyama WM, MHC class I alloantigen specificity of Ly-49^{+} IL-2 activated natural killer cells. Nature 358, 66–70 (1992). [PubMed: 1614533]

17. Moretta A, Bottino C, Vitale M, Pende D, Biassoni R, Mingari MC, Moretta L, Receptors for HLA class-I molecules in human natural killer cells. Ann. Rev. Immunol. 14, 619–648 (1996). [PubMed: 8717527]

18. Raulet DH, Vance RE, Self-tolerance of natural killer cells. Nat Rev Immunol 6, 520–531 (2006). [PubMed: 16799471]

19. Barry KC, Hsu J, Broz ML, Cueto FJ, Binnewies M, Combes AJ, Nelson AE, Loo K, Kumar R, Rosenblum MD, Alvarado MD, Wolf DM, Bogunovic D, Bhardwaj N, Daud AI, Ha PK, Ryan WR, Pollack JL, Samad B, Asthana S, Chan V, Krummel MF, A natural killer-dendritic cell axis defines checkpoint therapy-responsive tumor microenvironments. Nat Med 24, 1178–1191 (2018). [PubMed: 29942093]

20. Bottcher JP, Bonavita E, Chakravarty P, Blees H, Cabeza-Cabrerizo M, Sammicheli S, Rogers NC, Sahai E, Zelenay S, Reis ESC, NK Cells Stimulate Recruitment of cDC1 into the Tumor Microenvironment Promoting Cancer Immune Control. Cell 172, 1022–1037 e1014 (2018). [PubMed: 29429633]

21. Chen Q, Sun L, Chen ZJ, Regulation and function of the cGAS-STING pathway of cytosolic DNA sensing. Nat Immunol 17, 1142–1149 (2016). [PubMed: 27648547]

22. Ishikawa H, Ma Z, Barber GN, STING regulates intracellular DNA-mediated, type I interferon-dependent innate immunity. Nature 461, 788–792 (2009). [PubMed: 19776740]

23. Diner EJ, Burdette DL, Wilson SC, Monroe KM, Kellenberger CA, Hyodo M, Hayakawa Y, Hammond MC, Vance RE, The innate immune DNA sensor cGAS produces a noncanonical cyclic dinucleotide that activates human STING. Cell Rep 3, 1355–1361 (2013). [PubMed: 23707065]

24. Ablasser A, Goldeck M, Cavlar T, Deimling T, Witte G, Rohl I, Hopfner KP, Ludwig J, Hornung V, cGAS produces a 2'−5'-linked cyclic dinucleotide second messenger that activates STING. Nature 498, 380–384 (2013). [PubMed: 23722158]

25. Lam AR, Le Bert N, Ho SS, Shen YJ, Tang ML, Xiong GM, Croxford JL, Koo CX, Ishii KJ, Akira S, Raulet DH, Gasser S, RAE1 ligands for the NKG2D receptor are regulated by STING-dependent DNA sensor pathways in lymphoma. Cancer Res 74, 2193–2203 (2014). [PubMed: 24590060]

26. Woo SR, Fuertes MB, Corrales L, Spranger S, Furdyna MJ, Leung MY, Duggan R, Wang Y, Barber GN, Fitzgerald KA, Alegre ML, Gajewski TF, STING-dependent cytosolic DNA sensing mediates innate immune recognition of immunogenic tumors. Immunity 41, 830–842 (2014). [PubMed: 25517615]

27. Marcus A, Mao AJ, Lensink-Vasan M, Wang L, Vance RE, Raulet DH, Tumor-Derived cGAMP Triggers a STING-Mediated Interferon Response in Non-tumor Cells to Activate the NK Cell Response. Immunity 49, 754–763 e754 (2018). [PubMed: 30332631]

28. Zhu Q, Man SM, Gurung P, Liu Z, Vogel P, Lamkanfi M, Kanneganti TD, Cutting edge: STING mediates protection against colorectal tumorigenesis by governing the magnitude of intestinal inflammation. J Immunol 193, 4779–4782 (2014). [PubMed: 25320273]

29. Luteijn RD, Zaver SA, Gowen BG, Wyman SK, Garelis NE, Onia L, McWhirter SM, Katibah GE, Corn JE, Woodward JJ, Raulet DH, SLC19A1 transports immunoreactive cyclic dinucleotides. Nature 573, 434–438 (2019). [PubMed: 31511694]

30. Ritchie C, Cordova AF, Hess GT, Bassik MC, Li L, SLC19A1 Is an Importer of the Immunotransmitter cGAMP. Mol Cell 75, 372–381 e375 (2019). [PubMed: 31126740]

31. Deng L, Liang H, Xu M, Yang X, Burnette B, Arina A, Li XD, Mauceri H, Beckett M, Darga T, Huang X, Gajewski TF, Chen ZJ, Fu YX, Weichselbaum RR, STING-Dependent Cytosolic DNA Sensing Promotes Radiation-Induced Type I Interferon-Dependent Antitumor Immunity in Immunogenic Tumors. Immunity 41, 843–852 (2014). [PubMed: 25517616]

32. Sivick KE, Desbien AL, Glickman LH, Reiner GL, Corrales L, Surh NH, Hudson TE, Vu UT, Francica BJ, Banda T, Katibah GE, Kanne DB, Leong JJ, Metchette K, Bruml JR, Ndubaku CO,

McKenna JM, Feng Y, Zheng L, Bender SL, Cho CY, Leong ML, van Elsas A, Dubensky TW Jr., McWhirter SM, Magnitude of Therapeutic STING Activation Determines CD8(+) T Cell-Mediated Anti-tumor Immunity. Cell Rep 25, 3074–3085 e3075 (2018). [PubMed: 30540940]

33. Corrales L, Glickman LH, McWhirter SM, Kanne DB, Sivick KE, Katibah GE, Woo SR, Lemmens E, Banda T, Leong JJ, Metchette K, Dubensky TW Jr., Gajewski TF, Direct Activation of STING in the Tumor Microenvironment Leads to Potent and Systemic Tumor Regression and Immunity. Cell Rep 11, 1018–1030 (2015). [PubMed: 25959818]
34. Francica BJ, Ghasemzadeh A, Desbien AL, Theodros D, Sivick KE, Reiner GL, Hix Glickman L, Marciscano AE, Sharabi AB, Leong ML, McWhirter SM, Dubensky TW Jr., Pardoll DM, Drake CG, TNFalpha and Radioresistant Stromal Cells Are Essential for Therapeutic Efficacy of Cyclic Dinucleotide STING Agonists in Nonimmunogenic Tumors. Cancer Immunol Res 6, 422–433 (2018). [PubMed: 29472271]
35. Demaria O, De Gassart A, Coso S, Gestermann N, Di Domizio J, Flatz L, Gaide O, Michielin O, Hwu P, Petrova TV, Martinon F, Modlin RL, Speiser DE, Gilliet M, STING activation of tumor endothelial cells initiates spontaneous and therapeutic antitumor immunity. Proc Natl Acad Sci U S A 112, 15408–15413 (2015). [PubMed: 26607445]
36. Fu J, Kanne DB, Leong M, Glickman LH, McWhirter SM, Lemmens E, Mechette K, Leong JJ, Lauer P, Liu W, Sivick KE, Zeng Q, Soares KC, Zheng L, Portnoy DA, Woodward JJ, Pardoll DM, Dubensky TW Jr., Kim Y, STING agonist formulated cancer vaccines can cure established tumors resistant to PD-1 blockade. Science translational medicine 7, 283ra252 (2015).
37. Curran E, Chen X, Corrales L, Kline DE, Dubensky TW Jr., Duttagupta P, Kortylewski M, Kline J, STING Pathway Activation Stimulates Potent Immunity against Acute Myeloid Leukemia. Cell Rep 15, 2357–2366 (2016). [PubMed: 27264175]
38. Swann JB, Hayakawa Y, Zerafa N, Sheehan KC, Scott B, Schreiber RD, Hertzog P, Smyth MJ, Type I IFN contributes to NK cell homeostasis, activation, and antitumor function. J Immunol 178, 7540–7549 (2007). [PubMed: 17548588]
39. Rodig SJ, Gusenleitner D, Jackson DG, Gjini E, Giobbie-Hurder A, Jin C, Chang H, Lovitch SB, Horak C, Weber JS, Weirather JL, Wolchok JD, Postow MA, Pavlick AC, Chesney J, Hodi FS, MHC proteins confer differential sensitivity to CTLA-4 and PD-1 blockade in untreated metastatic melanoma. Science translational medicine 10, (2018).
40. Sade-Feldman M, Jiao YJ, Chen JH, Rooney MS, Barzily-Rokni M, Eliane JP, Bjorgaard SL, Hammond MR, Vitzthum H, Blackmon SM, Frederick DT, Hazar-Rethinam M, Nadres BA, Van Seventer EE, Shukla SA, Yizhak K, Ray JP, Rosebrock D, Livitz D, Adalsteinsson V, Getz G, Duncan LM, Li B, Corcoran RB, Lawrence DP, Stemmer-Rachamimov A, Boland GM, Landau DA, Flaherty KT, Sullivan RJ, Hacohen N, Resistance to checkpoint blockade therapy through inactivation of antigen presentation. Nat Commun 8, 1136 (2017). [PubMed: 29070816]
41. Zaretsky JM, Garcia-Diaz A, Shin DS, Escuin-Ordinas H, Hugo W, Hu-Lieskovan S, Torrejon DY, Abril-Rodriguez G, Sandoval S, Barthly L, Saco J, Homet Moreno B, Mezzadra R, Chmielowski B, Ruchalski K, Shintaku IP, Sanchez PJ, Puig-Saus C, Cherry G, Seja E, Kong X, Pang J, Berent-Maoz B, Comin-Anduix B, Graeber TG, Tumeh PC, Schumacher TN, Lo RS, Ribas A, Mutations Associated with Acquired Resistance to PD-1 Blockade in Melanoma. N Engl J Med 375, 819–829 (2016). [PubMed: 27433843]
42. Narni-Mancinelli E, Chaix J, Fenis A, Kerdiles YM, Yessaad N, Reynders A, Gregoire C, Luche H, Ugolini S, Tomasello E, Walzer T, Vivier E, Fate mapping analysis of lymphoid cells expressing the NKp46 cell surface receptor. Proc Natl Acad Sci U S A 108, 18324–18329 (2011). [PubMed: 22021440]
43. Jamieson AM, Diefenbach A, McMahon CW, Xiong N, Carlyle JR, Raulet DH, The role of the NKG2D immunoreceptor in immune cell activation and natural killing. Immunity 17, 19–29. (2002). [PubMed: 12150888]
44. Meric-Bernstam F, Sandhu SK, Hamid O, Spreafico A, Kasper S, Dummer R, Shimizu T, Steeghs N, Lewis N, Talluto CC, Dolan S, Bean A, Brown R, Trujillo D, Nair N, Luke JJ, Phase Ib study of MIW815 (ADU-S100) in combination with spartalizumab (PDR001) in patients (pts) with advanced/metastatic solid tumors or lymphomas. Journal of Clinical Oncology 37, 2507–2507 (2019).

45. Montoya M, Schiavoni G, Mattei F, Gresser I, Belardelli F, Borrow P, Tough DF, Type I interferons produced by dendritic cells promote their phenotypic and functional activation. Blood 99, 3263–3271 (2002). [PubMed: 11964292]
46. Diamond MS, Kinder M, Matsushita H, Mashayekhi M, Dunn GP, Archambault JM, Lee H, Arthur CD, White JM, Kalinke U, Murphy KM, Schreiber RD, Type I interferon is selectively required by dendritic cells for immune rejection of tumors. J Exp Med 208, 1989–2003 (2011). [PubMed: 21930769]
47. Mortier E, Woo T, Advincula R, Gozalo S, Ma A, IL-15R{alpha} chaperones IL-15 to stable dendritic cell membrane complexes that activate NK cells via trans presentation. J Exp Med 205, 1213–1225 (2008). [PubMed: 18458113]
48. Becknell B, Caligiuri MA, Interleukin-2, interleukin-15, and their roles in human natural killer cells. Adv Immunol 86, 209–239 (2005). [PubMed: 15705423]
49. Diefenbach A, Jamieson AM, Liu SD, Shastri N, Raulet DH, Ligands for the murine NKG2D receptor: expression by tumor cells and activation of NK cells and macrophages. Nat Immunol 1, 119–126 (2000). [PubMed: 11248803]
50. Hsu J, Hodgins JJ, Marathe M, Nicolai CJ, Bourgeois-Daigneault MC, Trevino TN, Azimi CS, Scheer AK, Randolph HE, Thompson TW, Zhang L, Iannello A, Mathur N, Jardine KE, Kirn GA, Bell JC, McBurney MW, Raulet DH, Ardolino M, Contribution of NK cells to immunotherapy mediated by PD-1/PD-L1 blockade. J Clin Invest 128, 4654–4668 (2018). [PubMed: 30198904]
51. Yang H, Lee WS, Kong SJ, Kim CG, Kim JH, Chang SK, Kim S, Kim G, Chon HJ, Kim C, STING activation reprograms tumor vasculatures and synergizes with VEGFR2 blockade. J Clin Invest 130, 4350–4364 (2019). [PubMed: 31343989]
52. Zitvogel L, Galluzzi L, Kepp O, Smyth MJ, Kroemer G, Type I interferons in anticancer immunity. Nat Rev Immunol 15, 405–414 (2015). [PubMed: 26027717]
53. Dunn GP, Koebel CM, Schreiber RD, Interferons, immunity and cancer immunoediting. Nat Rev Immunol 6, 836–848 (2006). [PubMed: 17063185]
54. Mizutani T, Neugebauer N, Putz EM, Moritz N, Simma O, Zebedin-Brandl E, Gotthardt D, Warsch W, Eckelhart E, Kantner HP, Kalinke U, Lienenklaus S, Weiss S, Strobl B, Muller M, Sexl V, Stoiber D, Conditional IFNAR1 ablation reveals distinct requirements of Type I IFN signaling for NK cell maturation and tumor surveillance. Oncoimmunology 1, 1027–1037 (2012). [PubMed: 23170251]
55. Degli-Esposti MA, Smyth MJ, Close encounters of different kinds: dendritic cells and NK cells take centre stage. Nat Rev Immunol 5, 112–124 (2005). [PubMed: 15688039]
56. Koka R, Burkett P, Chien M, Chai S, Boone DL, Ma A, Cutting edge: murine dendritic cells require IL-15R alpha to prime NK cells. J Immunol 173, 3594–3598 (2004). [PubMed: 15356102]
57. Mortier E, Advincula R, Kim L, Chmura S, Barrera J, Reizis B, Malynn BA, Ma A, Macrophage- and dendritic-cell-derived interleukin-15 receptor alpha supports homeostasis of distinct CD8+ T cell subsets. Immunity 31, 811–822 (2009). [PubMed: 19913445]
58. Lucas M, Schachterle W, Oberle K, Aichele P, Diefenbach A, Dendritic cells prime natural killer cells by trans-presenting interleukin 15. Immunity 26, 503–517 (2007). [PubMed: 17398124]
59. Mlecnik B, Bindea G, Angell HK, Sasso MS, Obenauf AC, Fredriksen T, Lafontaine L, Bilocq AM, Kirilovsky A, Tosolini M, Waldner M, Berger A, Fridman WH, Rafii A, Valge-Archer V, Pages F, Speicher MR, Galon J, Functional network pipeline reveals genetic determinants associated with in situ lymphocyte proliferation and survival of cancer patients. Science translational medicine 6, 228ra237 (2014).
60. Zhang Q, Bi J, Zheng X, Chen Y, Wang H, Wu W, Wang Z, Wu Q, Peng H, Wei H, Sun R, Tian Z, Blockade of the checkpoint receptor TIGIT prevents NK cell exhaustion and elicits potent anti-tumor immunity. Nat Immunol 19, 723–732 (2018). [PubMed: 29915296]
61. Meazza R, Azzarone B, Orengo AM, Ferrini S, Role of common-gamma chain cytokines in NK cell development and function: perspectives for immunotherapy. J Biomed Biotechnol 2011, 861920 (2011).
62. Ardolino M, Azimi CS, Iannello A, Trevino TN, Horan L, Zhang L, Deng W, Ring AM, Fischer S, Garcia KC, Raulet DH, Cytokine therapy reverses NK cell anergy in MHC-deficient tumors. J Clin Invest 124, 4781–4794 (2014). [PubMed: 25329698]

63. Deng W, Gowen BG, Zhang L, Wang L, Lau S, Iannello A, Xu J, Rovis TL, Xiong N, Raulet DH, Antitumor immunity. A shed NKG2D ligand that promotes natural killer cell activation and tumor rejection. Science 348, 136–139 (2015). [PubMed: 25745066]

64. Thompson TW, Kim AB, Li PJ, Wang J, Jackson BT, Huang KTH, Zhang L, Raulet DH, Endothelial cells express NKG2D ligands and desensitize anti-tumor NK responses. Elife 6, e30881 (2017).

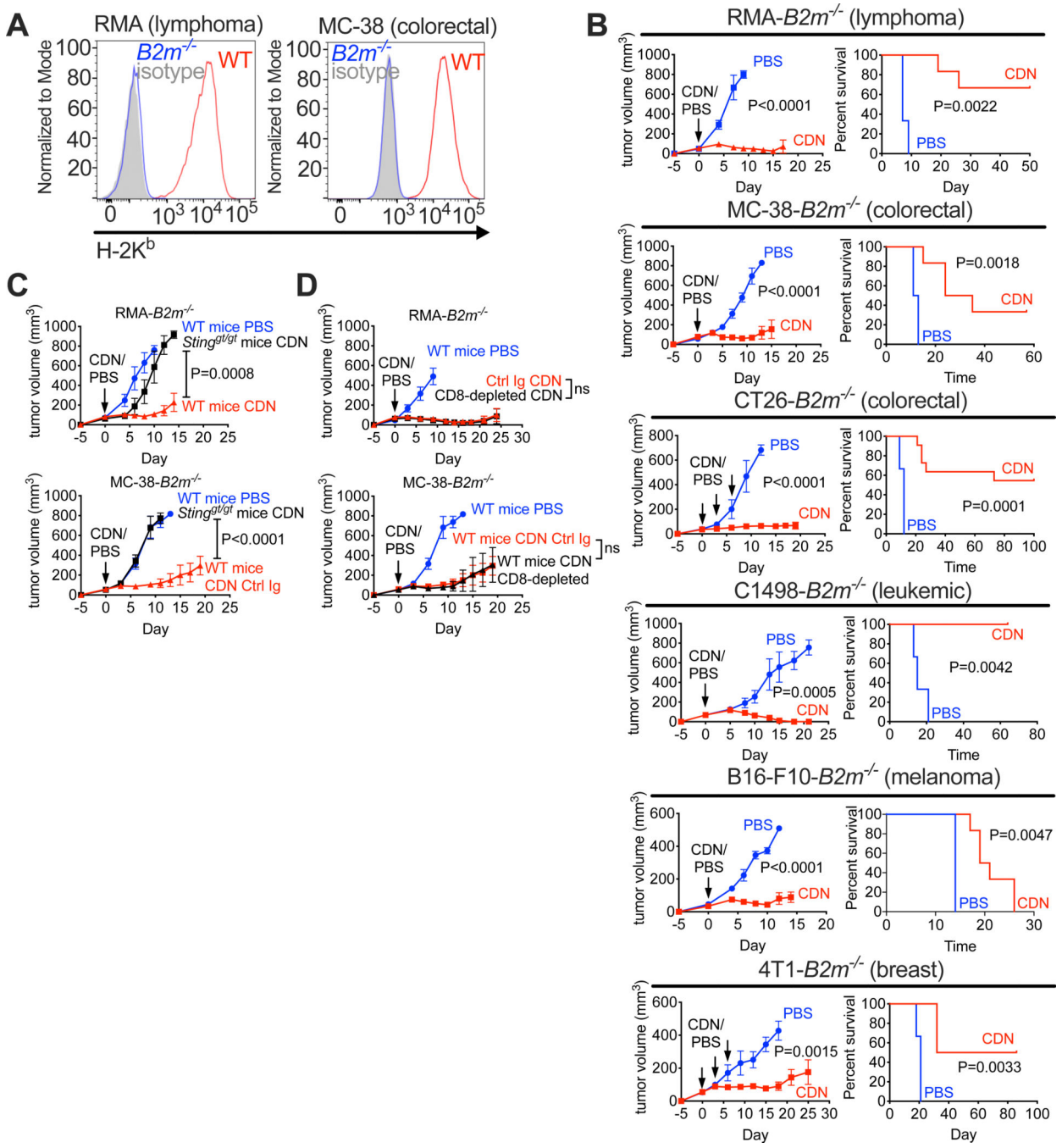

Fig. 1. Rejection of MHC I-deficient tumors induced by intratumoral injections of CDN (2'3' RR c-di-AMP).

(**A**) WT and *B2m*$^{-/-}$ tumor cells were stained with MHC class I (H-2K^{b} clone AF6–88.5) or isotype control antibodies. (**B**) Tumor cells were injected s.c. in C57BL/6J or BALB/c (CT26 and 4T1) mice and treated i.t. 5 days later with PBS or once with 50 μg of CDN, or three times with 25 μg CDN over 5 days, indicated by the arrows. Tumor volume and survival was analyzed with 2-way ANOVA and log-rank (Mantel-Cox) tests, respectively. n=5–11 for CDN-treated mice and 3–4 for PBS-treated mice. Data are representative of 2

independent experiments. (**C**) Tumors were established in C57BL/6J or *Sting*$^{gt/gt}$ mice, treated, and analyzed as in B. n=6 for CDN/WT groups and 3–4 for the other groups. Data are representative of 2 independent experiments. (**D**) Tumors were established, treated, and analyzed as in B. Mice were CD8-depleted or received control rat Ig (see Methods). n=5–8 for the CDN-treated groups and 3–4 for the PBS-treated group. Data are representative of 2 independent experiments. For the MC-38 data in Figures C and D, the PBS-treated and CDN Ctrl Ig-treated growth curves were from the same experiment and are shown in both panels.

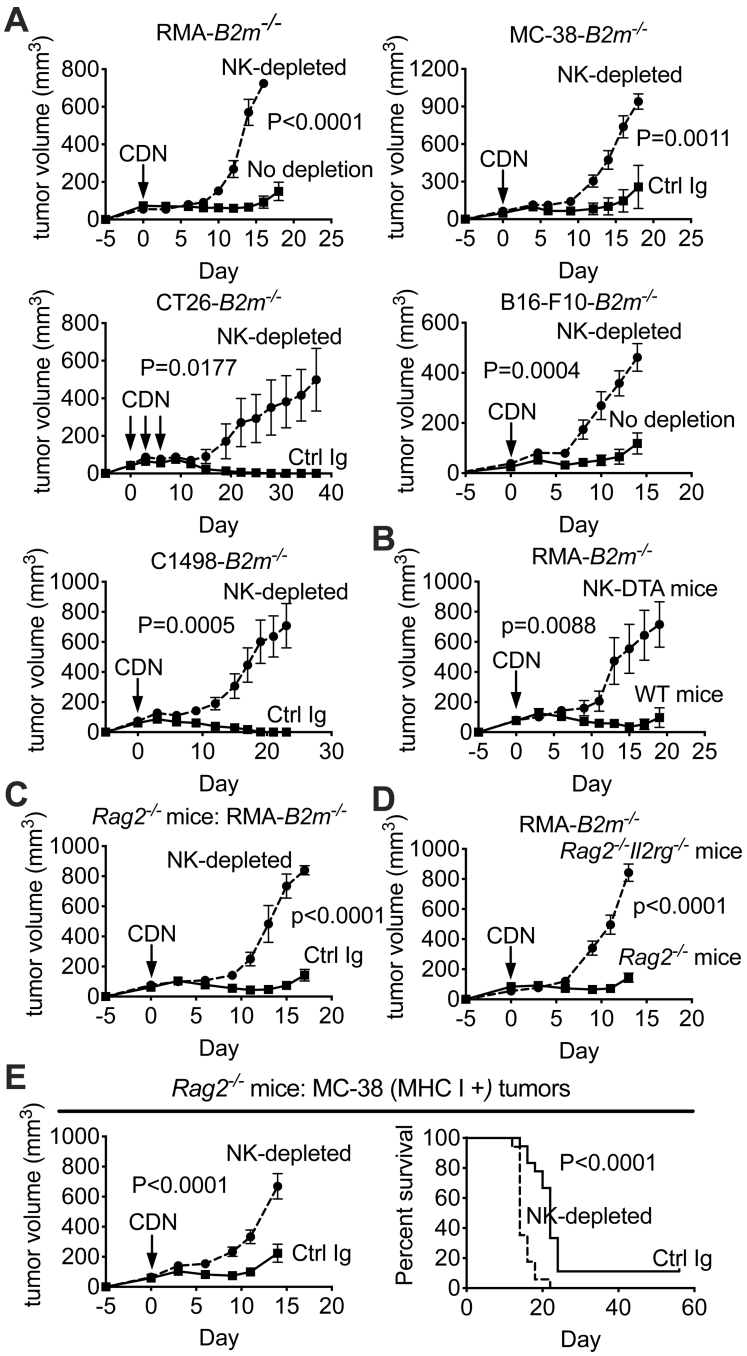

Fig. 2. NK-dependence of tumor rejection induced by CDNs.

(**A**) C57BL/6J or BALB/c (CT26 and 4T1 tumors), (**B**) NK-DTA, (**C**-**D**) *Rag2*$^{-/-}$ or (**D**) *Rag2*$^{-/-}$*Il2rg*$^{-/-}$ mice were injected s.c. with tumor cells of the types indicated and tumors were allowed to establish for 5 days. In some experiments (**A**, **C**, **E**) mice were NK-depleted (see Methods). Tumors were treated and analyzed as described in Fig. 1B. (**E**) *B2m*$^{+/+}$ MC-38 tumors (MHC I^{+}) were established in *Rag2*$^{-/-}$ mice that were NK-depleted or not, CDN-treated, and analyzed as in Fig. 1B. For Fig. A-D, data representative of 2–3

independent experiments. n=5–9. For Fig. E, data was combined from 3 independent experiments. n=18.

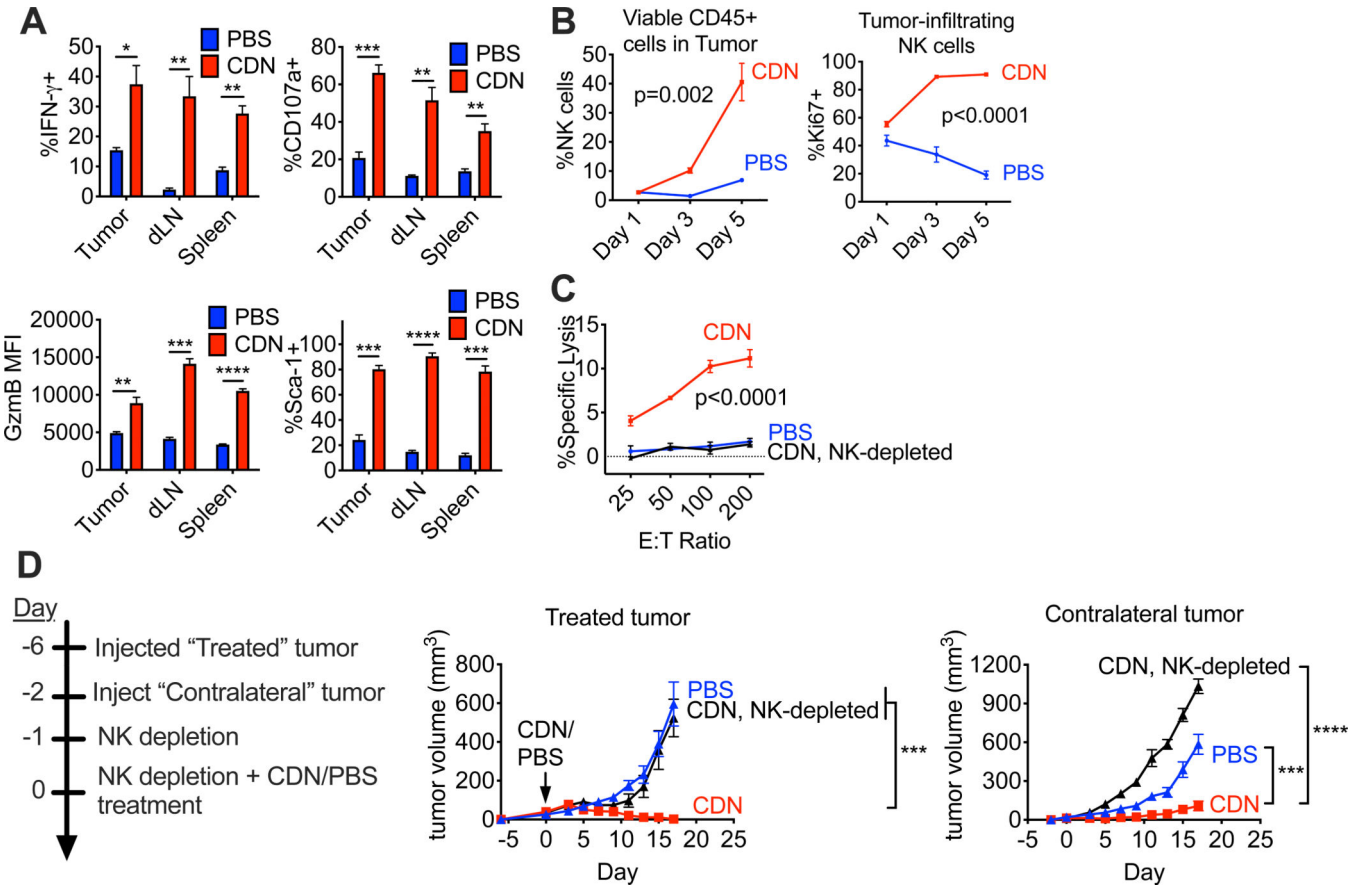

Fig. 3. Activation, proliferation and cytotoxicity of NK cells induced by CDN treatments of tumors.

(**A**) RMA-*B2m*$^{-/-}$ tumors were established and treated as in Fig. 1B. 24 h later tumors, tumor-draining lymph nodes, and spleens were harvested and stained for flow cytometry. NK cells were gated as viable, CD45^{+}, CD3^{-}, CD19^{-}, F4/80^{-}, Ter119^{-}, NK1.1^{+}, NKp46^{+} cells. n=3. 2-tailed unpaired Student's t-tests with the Holm-Sidak method for multiple comparisons was used. *P<0.05; **P<0.01; ***P < 0.001, ****P<0.0001. Data are representative of 2 independent experiments. (**B**) RMA-*B2m*$^{-/-}$ tumors were established, treated, harvested, stained and analyzed on the days indicated. n=3. Data are representative of 2 independent experiments and analyzed with 2-way ANOVA. Error bars are shown but may be too small to see. (**C**) RMA-*B2m*$^{-/-}$ tumors were established and treated as in Fig. 1B. 24 h after treatment, splenocytes were harvested and identical groups were pooled. Some groups were NK-depleted (see Methods). Cytotoxicity against RMA-*B2m*$^{-/-}$ target cells was performed in technical triplicate and error bars are shown but are typically too small to see. Data (representative of two independent experiments) were analyzed by 2-way ANOVA. (**D**) Experimental schematic is shown. C1498-*B2m*$^{-/-}$ tumors were established in both flanks of *Rag2*$^{-/-}$ mice 4 days apart at a dose of 4×10^{6} cells each. One day after the second, "contralateral", tumor was established, NK cells were depleted as in Methods. NK cells were depleted again the next day and weekly thereafter. 6 days after the first, "Treated", tumor was established, it was treated with PBS or 50 μg CDN. Tumor growth at both sites

was monitored and analyzed as described in Fig. 1B. Data (combined from two independent experiments) were analyzed by 2-way ANOVA. ***P < 0.001, ****P<0.0001. n=6–8.

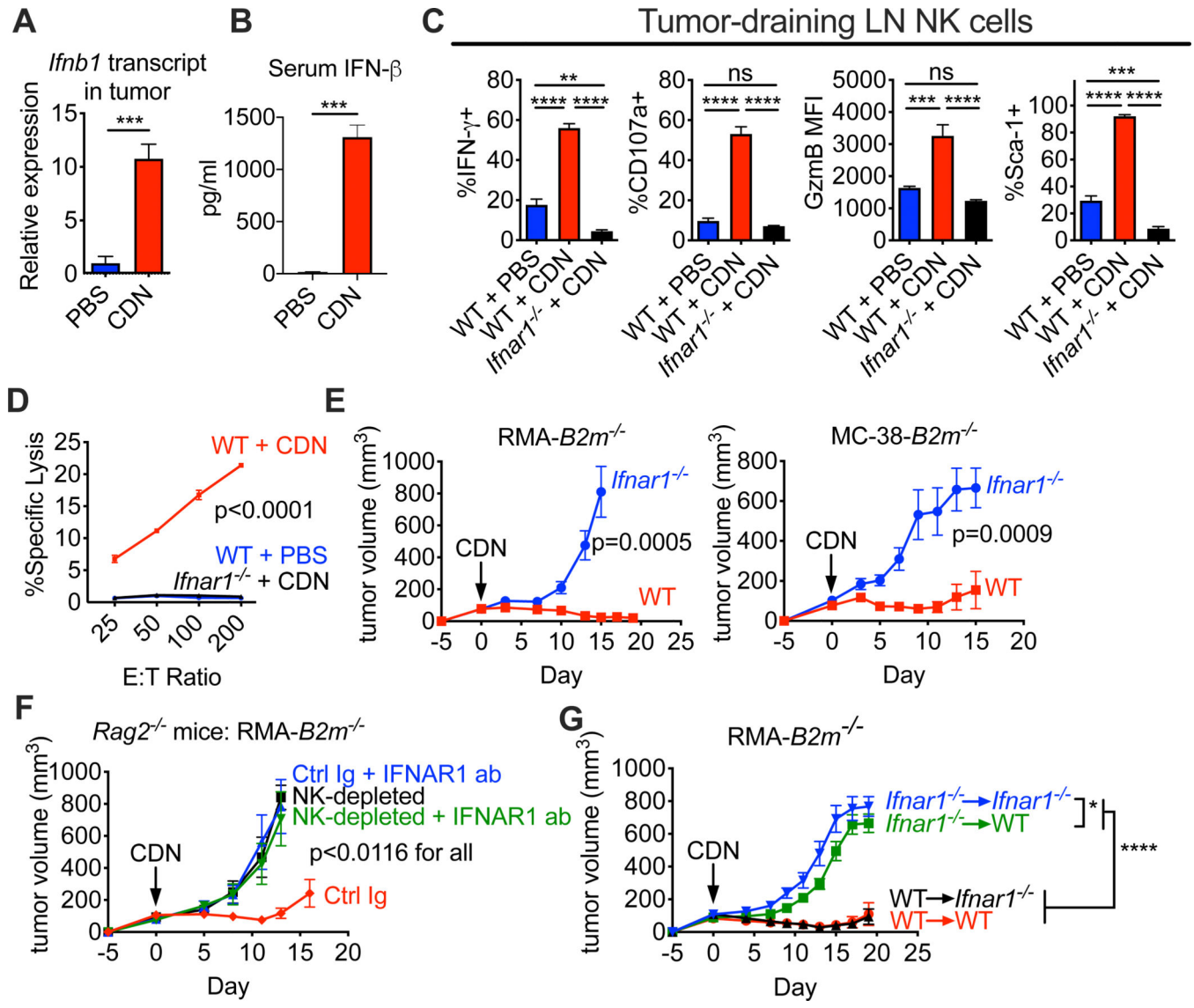

Fig. 4. Critical role for type I interferons in the NK-dependent tumor rejection response induced by CDNs.

(**A**) RMA-*B2m*$^{-/-}$ tumors were established and treated as described in Fig. 1B. 24 hours later tumors were harvested, RNA extracted, and qRT-PCR performed to quantify *Ifnb1* transcripts. n=4. ***P < 0.001, as analyzed by 2-tailed unpaired Student's t-test. Data are representative of 2 independent experiments. (B) RMA-*B2m*$^{-/-}$ tumors were established and treated as described in Fig. 1B. 6 hours later serum was collected and IFN-β was quantified by ELISA. ***P<0.001, as analyzed by Mann Whitney test. Data are combined from two independent experiments. n=8. (**C**) RMA-*B2m*$^{-/-}$ tumors were established and treated as described in Fig.1B. 24 h later tumor-draining lymph node cells were harvested for flow cytometry analysis as in Fig. 3A. n=5. **P<0.01; ***P < 0.001; ****P<0.0001, as analyzed by one-way ANOVA with Tukey's correction for multiple comparisons. Data are representative of 2 independent experiments. (**D**) Cytotoxicity of splenocytes from tumor-bearing, PBS or CDN-treated mice analyzed as in Fig. 3C. Data are representative of two

independent experiments. Error bars are shown but are typically too small to see. (**E**) Tumors were established in C57BL/6J or *Ifnar1*$^{-/-}$ mice, treated, and analyzed as in Fig. 1B. n=5–6. Data are representative of two independent experiments. (**F**) RMA-*B2m*$^{-/-}$ tumors were established in *Rag2*$^{-/-}$ mice and treated and analyzed as in Fig. 1B. Some animals were depleted of NK cells and/or given IFNAR1 neutralizing antibody (see Methods). Data are representative of two independent experiments. (G) Bone marrow chimeras were established with the indicated donor → recipient combinations of C57BL/6J and *Ifnar1*$^{-/-}$ bone marrow (see Methods). Eight weeks later, RMA-*B2m*$^{-/-}$ tumors were established, treated, and analyzed as in Fig. 1B. n=8–12 per group.

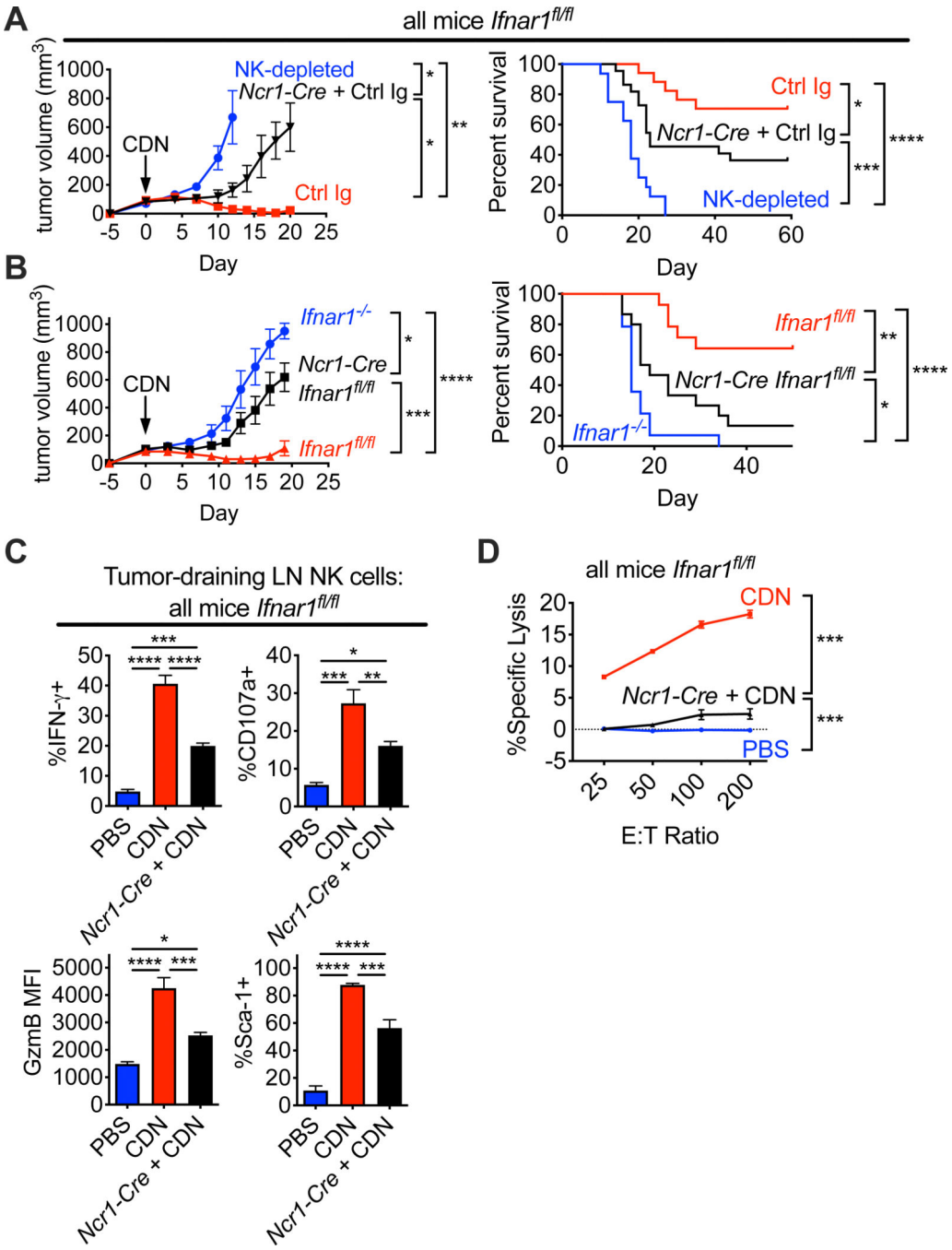

Fig. 5.

Interferon acts directly on NK cells to mediate therapeutic effects of CDN treatments. (**A-B**) RMA-*B2m*$^{-/-}$ tumors were established in the indicated genotypes, treated, and analyzed as in Fig. 1B. NK depletions were performed as described in Methods. Data are representative of 2–3 independent experiments. n=4–8. Survival data is combined from 2–3 experiments (n=14–22 per group). (**C**) RMA-*B2m*$^{-/-}$ tumors were established in the indicated genotypes and treated as before. 24 h later tumor-draining lymph node cells were harvested for flow cytometry as in Fig. 3A. n=4–6. Data (representative of 2 independent experiments) were

analyzed with one-way ANOVA with Tukey's correction for multiple comparisons. *P < 0.05; **P<0.01; ***P < 0.001; ****P<0.0001. (**D**) Cytotoxicity of splenocytes from tumor-bearing PBS or CDN-treated mice of the indicated genotypes analyzed as in Fig. 3C. Data are representative of two independent experiments. ***P < 0.001. Error bars are shown but are typically too small to see.

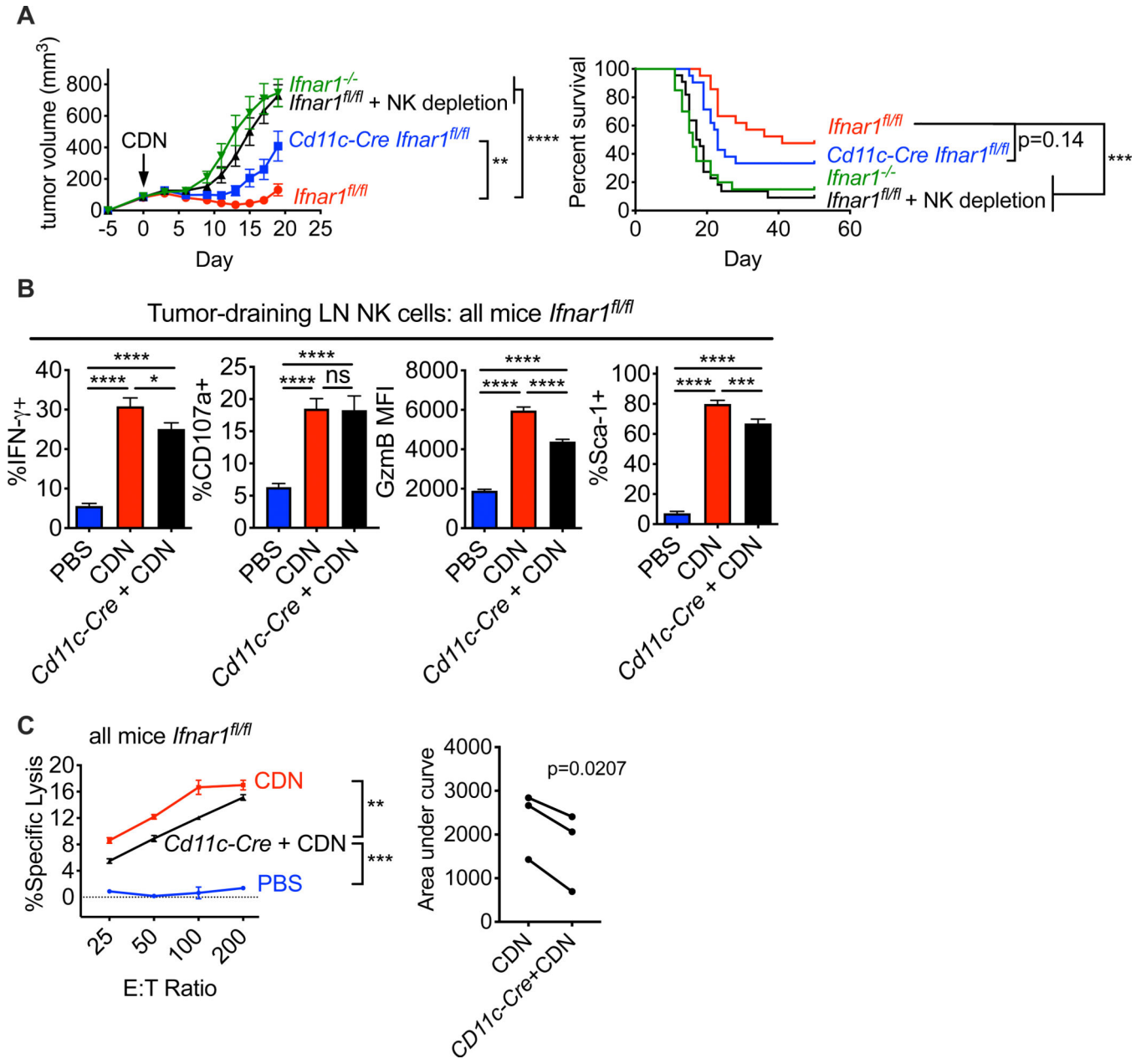

Fig. 6. Interferon acts on dendritic cells to enhance NK cell activation and tumor rejection induced by CDN therapy.

(**A**) RMA-*B2m*$^{-/-}$ tumors were established in the indicated genotypes, treated, and analyzed as in Fig. 1B. NK depletion was performed as described in Methods. Tumor growth data are combined from 2 experiments (n=15–16 per group). Survival data are combined from 3 experiments (n=20–21 per group). **P<0.01; ***P < 0.001; ****P<0.0001. (**B**) RMA-*B2m*$^{-/-}$ tumors were established in the indicated genotypes and treated as before. 24 h later, flow cytometric analysis of tumor-draining LN NK cells was performed as in Fig. 3A. n=17–22. *P < 0.05; **P<0.01; ***P < 0.001; ****P<0.0001 as analyzed with one-way ANOVA tests with Tukey's correction for multiple comparisons or Kruskal-Wallis with Dunn's multiple comparisons test for nonparametric data. Data are combined from 4 independent

experiments. (**C**) Cytotoxicity of splenocytes from tumor-bearing PBS or CDN-treated mice of the indicated genotypes were analyzed as in Fig. 3C. **P<0.01; ***P < 0.001. Error bars are shown but are typically too small to see. One experiment is shown in the left panel and the reduced killing from *Cd11c-Cre, Ifnar1*$^{fl/fl}$ splenocytes was confirmed in a total of 3 independent experiments where the areas under the cytotoxicity curves were compared using paired, 2-tailed Student's t-tests (right panel).

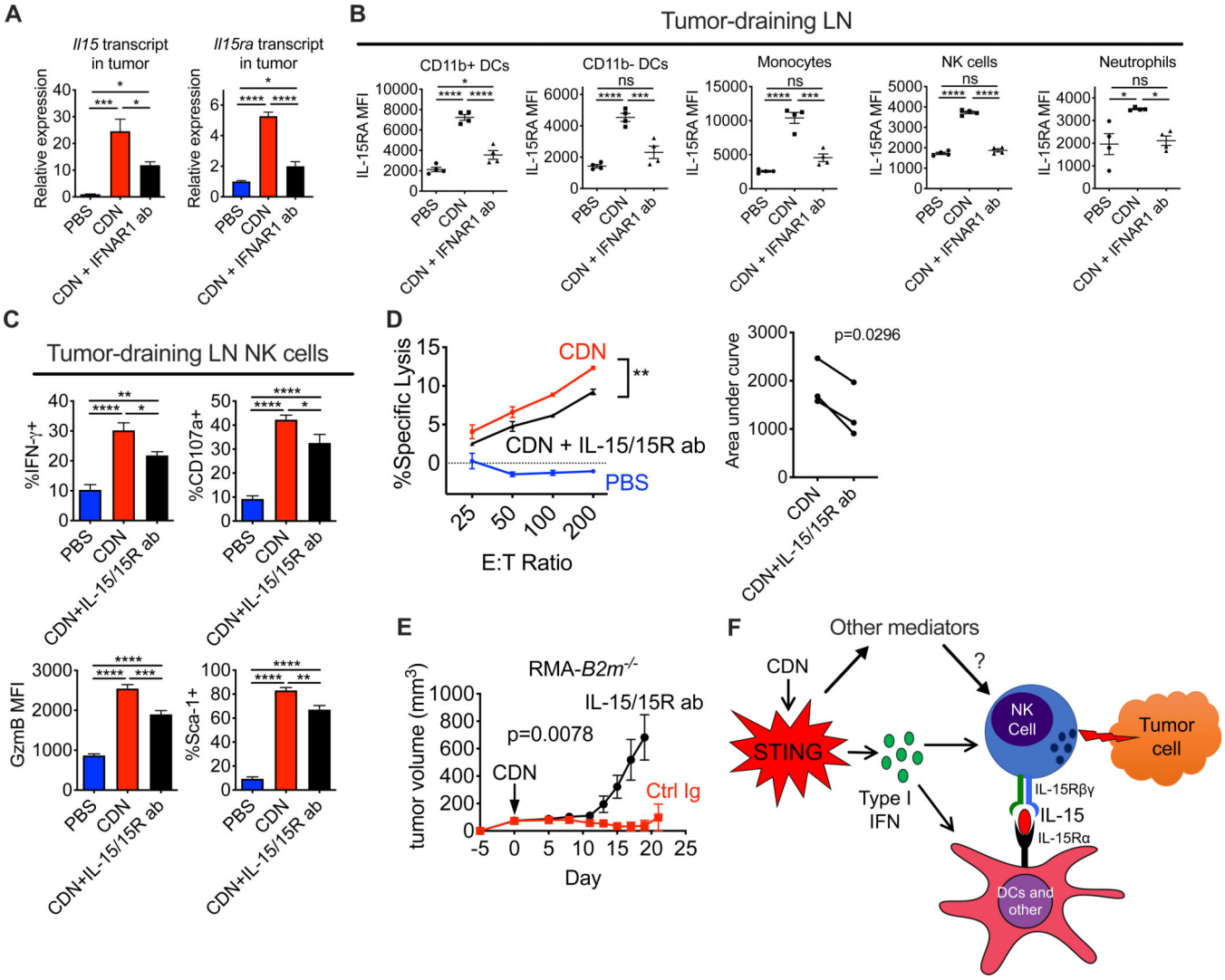

Fig. 7. IL-15/IL-15Rα expression is induced on DCs and other cells by interferons after CDN therapy and contributes significantly to optimal NK cell activation and tumor rejection.

(**A**) RMA-*B2m*$^{-/-}$ tumors were established, treated, RNA-extracted, and analyzed by qPCR for *Il15* or *1l15ra* transcripts as in Fig. 4A. Some mice received IFNAR1 neutralizing antibody (see Methods). n=4. Data (representative of 2 independent experiments) were analyzed with one-way ANOVA with Tukey's correction for multiple comparisons. (**B**) RMA-*B2m*$^{-/-}$ tumors were established and treated as before. 24 h later tumor-draining lymph node cells were harvested for flow cytometry as in Methods. The mean fluorescence intensity (MFI) of IL-15RA (BAF551) is displayed. Viable CD3^{-}, CD19^{-}, Ter119^{-} cells were further gated on DCs (NK1.1^{-}, Ly6G^{-}, CD11c^{high}, MHC-II^{high}), monocytes (NK1.1^{-}, Ly6G^{-}, CD11b^{high}, Ly6C^{high}), neutrophils (NK1.1^{-}, CD11b^{+}, Ly6G^{+}), NK cells (NK1.1^{+}), and macrophages (NK1.1^{-}, Ly6G^{-}, CD11b^{+}, F4/80^{+}). n=4. **P<0.01; ***P < 0.001; ****P<0.0001, as analyzed by one-way ANOVA with Tukey's correction for multiple comparisons. Data are representative of 2 independent experiments. (**C**) RMA-*B2m*$^{-/-}$ tumors were established, treated, and tumor-draining LN NKs were analyzed by flow cytometry as in Fig. 3A. Some mice received IL-15/IL-15R neutralizing antibody (see

Methods). n=5. **P<0.01; ***P < 0.001; ****P<0.0001. Data (representative of 2 independent experiments) were analyzed with one-way ANOVA with Tukey's correction for multiple comparisons. (**D**) Cytotoxicity of splenocytes from tumor-bearing PBS or CDN-treated mice were analyzed as in Fig. 3C. Some mice received IL-15/IL-15R neutralizing antibody or control Ig (see Methods). **P<0.01. Error bars shown but typically too small to see. One experiment is shown in the left panel and the reduced killing from IL-15R neutralization was confirmed in a total of three independent experiments where the areas under the cytotoxicity curves were compare using paired, 2-tailed Student's t-tests (right panel). (**E**) RMA-*B2m*$^{-/-}$ tumors were established, treated, and analyzed as in Fig. 1B. Mice received 5 μg IL-15/IL-15R antibody or control IgG (see Methods). n=5 per group. Data are representative of 2 independent experiments. (**F**) Model of CDN-induced NK cell activation. I.t. CDN treatment activates the STING pathway, resulting in production of type I IFN and other mediators including cytokines and chemokines, boosting NK cell effector functions and antitumor activities. Type I IFN elicits its effects on NK cells by direct action and indirectly via DCs, which upregulate IL-15/IL-15Rα complexes to enhance NK cell antitumor effects.